



This is a repository copy of *A neighbourhood-level analysis of the impact of common urban forms on energy use in drinking water distribution systems*.

White Rose Research Online URL for this paper:  
<https://eprints.whiterose.ac.uk/162335/>

Version: Accepted Version

---

**Article:**

Wong, H., Filion, Y.R. and Speight, V. (2020) A neighbourhood-level analysis of the impact of common urban forms on energy use in drinking water distribution systems. *Water Resources Management*, 34. pp. 2641-2655. ISSN 0920-4741

<https://doi.org/10.1007/s11269-020-02511-w>

---

This is a post-peer-review, pre-copyedit version of an article published in *Water Resources Management*. The final authenticated version is available online at:  
<http://dx.doi.org/10.1007/s11269-020-02511-w>.

**Reuse**

Items deposited in White Rose Research Online are protected by copyright, with all rights reserved unless indicated otherwise. They may be downloaded and/or printed for private study, or other acts as permitted by national copyright laws. The publisher or other rights holders may allow further reproduction and re-use of the full text version. This is indicated by the licence information on the White Rose Research Online record for the item.

**Takedown**

If you consider content in White Rose Research Online to be in breach of UK law, please notify us by emailing [eprints@whiterose.ac.uk](mailto:eprints@whiterose.ac.uk) including the URL of the record and the reason for the withdrawal request.



[eprints@whiterose.ac.uk](mailto:eprints@whiterose.ac.uk)  
<https://eprints.whiterose.ac.uk/>

1  
2 **A Neighbourhood-Level Analysis of the Impact of Common Urban Forms On**  
3 **Energy Use in Drinking Water Distribution Systems**

4 Hannah G. Wong<sup>1</sup>, Yves R. Filion<sup>2</sup>, Vanessa L. Speight<sup>3</sup>

5 **Abstract**

6 This paper examined the link between common urban forms in North America and the energy  
7 use of drinking water distribution systems. (The urban form of an urban area relates to its street  
8 topology and population density.) Common street topologies and neighborhood population  
9 densities were combined to evaluate the impact on pumping energy and embodied energy in  
10 drinking water distribution systems. Embodied energy included the life-cycle activities required  
11 for the fabrication, transportation, and initial installation of pipes. The results indicated that the  
12 gridiron topology had a lower embodied and pumping energy use than the warped parallel and  
13 cul-de-sac/loop topologies. The high population density associated with the gridiron topology  
14 produced a lower per capita water demand and pumping energy use.

15  
16 *Keywords:* water supply and distribution systems; urban form; water demand; pipe flow;  
17 embodied energy, pumping energy.

18  
19  
20  
21  
22  
23 <sup>1</sup> Hannah Wong, Owner, *Luminous Ground Farm*, Peterborough, Ontario, Canada.

24 <sup>2</sup> Yves R. Filion, Professor, Queen's University, Kingston, Ontario, Canada, K7L 3N6 (e-mail:  
25 [yves.filion@queensu.ca](mailto:yves.filion@queensu.ca)).

26 <sup>3</sup> Vanessa Speight, Senior Research Fellow, University of Sheffield, Sheffield, UK, S1 3JD, (e-  
27 mail: [v.speight@sheffield.ac.uk](mailto:v.speight@sheffield.ac.uk)).

29 **Introduction**

30 Post war development and urban planning policies have encouraged the sprawling of US and  
31 Canadian cities (Southworth and Owens 1993). Cities and their underlying water infrastructure  
32 have become more spatially diffuse in the last 70 years. Drinking water systems in particular  
33 have evolved in a similar manner as the road system and urban fabric of major metropolitan  
34 areas. The distance needed to pump water from source to user has only increased in the  
35 intervening decades of urban development. Indeed, Goldstein and Smith (2002) and Sanders and  
36 Webber (2012) have reported that 4-12% of electricity use in the US is devoted to the  
37 distribution and treatment of water and wastewater. This is hardly surprising given that water is  
38 heavy with a density of  $1000 \text{ kg/m}^3$  and requires a large amount of energy to convey through  
39 pipes with operating pressures ranging between 200-700 kPa. Outside of their operating  
40 requirements, water supply and distribution systems also represent a large initial outlay of  
41 materials and energy to construct. Prosser et al. (2013) reported large initial embodied energy  
42 costs required to fabricate, transport, and install pipes, pumps, and tanks and other components in  
43 these systems. The items above point to a need to examine how the geographic shape of  
44 neighborhoods and population densities affect the energy use to fabricate and operate drinking  
45 water systems.

46  
47 To document the physical evolution of urban environments, Southworth and Owens (1993)  
48 identified neighbourhood street patterns (street topologies) commonly found in North America  
49 over the last century (Figure 1). The evolution of street patterns over time is in response to  
50 changes in the social, economic, and technological environment. The gridiron topology  
51 comprises many intersections and points of access, maximizing the number of possible routes  
52 and minimizing trip lengths. This pattern was most common in the early 1900s, when  
53 transportation occurred mostly on foot. With the rise of the car as the principal mode of travel,  
54 street design was adjusted accordingly with longer blocks and fewer intersections, as seen in the  
55 fragmented parallel pattern. Urban planning ideals of the time also sought to emulate more  
56 “rural” and “natural” landscapes, resulting in curving streets and more self-contained  
57 neighbourhoods. This is most clearly seen in the warped parallel topology of the 1960s. Street  
58 patterns in the 1970s and onward departed from the gridiron structure entirely. Cul-de-sacs and  
59 small loops were used to maximize privacy by decreasing connectivity and reducing through-

60 traffic. As a result, these neighbourhoods comprise very few access points, and route choices in  
61 these neighbourhoods are limited (Southworth and Owens 1993).

62  
63 Urban form has also been connected to the variation in residential per capita water use. Sakrison  
64 (1997) found that in the Seattle metropolitan area, higher density, gridiron neighbourhoods used  
65 less water than conventional suburban developments. Domene and Sauri (2006) found that in the  
66 metropolitan region of Barcelona, household size and housing type played a significant role in  
67 determining water use. Low-density, single-family homes tended to consume more water  
68 because of increased outdoor water uses. Similarly, outdoor water use in North America has been  
69 found to be much higher in neighbourhoods with lower densities and larger irrigable areas  
70 (Friedman et al. 2013, Van Lare 2005).

71  
72 There has been a recent interest in examining the impact of urban form on the performance of  
73 water infrastructure systems in the urban environment. Jia et al. (2019) examined a number of  
74 wastewater and rainwater systems situated in different urban forms and evaluated their  
75 performance in terms of economic efficiency, effectiveness and adaptability. They found that  
76 urban form has a larger impact on the performance of rainwater systems than it does on the  
77 performance of wastewater systems. Huang et al. (2018) examined the impact of factors such as  
78 geographic differences and city forms on the energy use in urban water supply systems in China.  
79 The authors found that the plane area ratio of a distribution network constrained by the physical  
80 layout of the urban environment had an influence on the energy use of water supply systems.  
81 Other factors such as the volume of water supplied and the leakage rate also were important  
82 factors to consider in the energy use of Chinese water supply systems. Farmani and Butler (2014)  
83 examined the urban form of a well-known benchmark distribution network and its economic and  
84 hydraulic performance. The authors surveyed a large number of urban growth rates, urban forms  
85 that included compact/uniform, monocentric, polycentric and edge forms, and water efficiency  
86 strategies and analyzed the benchmark network in terms of total cost, resilience, and water  
87 quality performance. The authors found that the urban form and the rate of growth had major  
88 implications for the cost and hydraulic performance of their distribution network.

89

90 Recently, researchers have examined the link between urban form and the energy use in water  
91 supply and distribution systems. Filion (2008) applied life-cycle energy analysis (LCEA) to  
92 calculate the energy required for pipe fabrication, pipe break repair, pumping, and pipe disposal  
93 in nine network configurations with different population distributions. Here, energy use was  
94 lower in compact and highly connected networks with dense population centres near the water  
95 source. In a follow-up study, Wong et al. (2017) examined the effect of urban development  
96 patterns on the energy use of a water distribution system in the US. The researchers found that  
97 lift energy was highest in zones located furthest from the river source and the frictional energy  
98 losses were highest in zones nearest the source. Surprisingly, the frictional energy loss in the  
99 zone nearest the source was comparable to those in zones near the edge of the system with a  
100 lower level of connectivity. In the urban intensification scenario considered by Wong et al.  
101 (2017), the reallocation of demand from the edge to the urban core of the system decreased  
102 energy use by 50%.

103

104 Both Filion (2008) and Wong et al. (2017) commented that since urban growth is incremental,  
105 city networks generally do not exhibit a single idealized spatial configuration (e.g., gridiron,  
106 radial, satellite). Instead, as cities grow and expand over the course of many decades, they  
107 become a patchwork of zones featuring different configurations (Filion 2008). As a result,  
108 analysis should be situated where the differences in urban form are found—at the level of the  
109 neighbourhood.

110

111 The aim of this paper is to examine the impact of urban form on pumping energy and embodied  
112 energy in distribution systems at the neighbourhood level. This paper seeks to address two  
113 pertinent research questions:

- 114 • How do street topologies affect energy use in a neighbourhood?
- 115 • How does population density affect energy use in a neighbourhood?

116

117 The paper makes an important research contribution to the area as it is the first paper to report a  
118 detailed examination of the impact of network topology and population density on the embodied  
119 and pumping energy use in water distribution systems at the neighbourhood level. Previous  
120 research in this area have only considered these relationships at the level of the entire network.

121

122 **Methods**

123 *Impact of Street Topology and Population Density on Energy Use*

124 Neighbourhood scenarios were created by combining different population density levels with  
125 traditional network topologies found in North American cities. A single per capita average water  
126 demand was used in all neighbourhood scenarios to isolate for the effects of topology and  
127 density. Each neighbourhood scenario was comprised of 750 lots each with a household density  
128 of three people/lot (Census 2015) and a population of 2,250 capita in each neighbourhood.

129

130 *Urban Form Variables—Topology and Population Density*

131 Three popular topologies—gridiron (GR), warped parallel (WP), and cul-de-sac/loop (CL)—were  
132 chosen for analysis and are based on the neighbourhood street patterns identified by Southworth  
133 and Owens (1993) (Figure 2). To analyze the impact of smaller physical variations within each  
134 topology, multiple neighbourhoods in each category were considered. For the gridiron (GR),  
135 warped parallel (WP), and cul-de-sac (CL) topologies, three real neighbourhoods were obtained  
136 from Google Earth (Google Inc. 2013) (Figure 2). For this study, population density was  
137 expressed as net density, which is defined as the number of lots divided by the land area that is  
138 used for residential purposes only. Net density does not consider the contribution of green space,  
139 roads, and other non-residential space within the neighbourhood to the measured total area. As a  
140 result, a variation in net density would be brought about by directly increasing or decreasing the  
141 size of residential lots. Lot area values at high, medium, and low densities were based on the  
142 urban planning guidelines of a US municipality (City of Miamisburg 2013). In order to apply  
143 these densities to each neighbourhood scenario, the length of each original network was scaled  
144 up or down to match the lot areas designated for each density.

145

146 Although this examination took a systematic approach to consider each combination of topology  
147 (GR, WP, CL) and density (high, medium, low), each topology is associated with a certain  
148 “native” density in reality. This is because the same social factors that drove the progression  
149 from gridiron to cul-de-sac/loop layouts also drove the progression from high to low density  
150 neighbourhoods (Southworth and Owens 1993). Barring the recent trend of decreasing density in  
151 the last few decades (Knaap et al. 2007), gridiron neighbourhoods tend to be associated with

152 higher densities while warped parallel and cul-de-sac/loop neighbourhoods have lower densities.  
153 This is reflected in the neighbourhood scenarios used for this investigation. Table 1 summarizes  
154 the lot area values for each density level as well as the base neighbourhoods associated with each  
155 density category.

156

### 157 *Embodied Energy and Pumping Energy*

158 The life-cycle energy analysis of Prosser et al. (2013) based on pipe length and diameter was  
159 used to quantify the embodied energy associated with each topology considered in the paper. For  
160 commercially-available diameters of ductile iron pipe ranging from 150-400 mm, Prosser et al.  
161 (2013) reported embodied energy per unit length of 342-789 kWh/m.

162

163 The pumping energy use in each neighborhood considered were determined by performing a  
164 steady-state hydraulic simulation with the EPANET2 network solver (Rossman 2000). Table 2  
165 summarizes the network parameters used in the models. Changes in elevation throughout the  
166 neighbourhood were not considered for two reasons. First, a constant elevation was used to  
167 isolate the effect of pipe topology and population density distribution on dynamic losses from  
168 friction in the neighborhood systems and removing the effect of static lift driven by changes in  
169 elevation or variable topography. Second, a constant elevation was imposed across all  
170 neighborhood systems to compare their energy use from dynamic losses only in a fair manner  
171 and without the effect of elevation and static lift. In reality, each neighborhood would have its  
172 unique topography and pumping energy requirement to overcome its corresponding static lift.  
173 The houses in each neighbourhood were assigned to the nearest network node in order to obtain  
174 the total water demand at each node. A per capita water consumption rate 400 litres per capita  
175 per day (lpcd) typical for North America was used (Environment Canada 2011, MOE 2008).  
176 Preliminary testing determined that pumping energy trends were difficult to ascertain at this  
177 magnitude of demand since all pipes in the model were set at a minimum diameter of 150 mm to  
178 accommodate large fire flows (Walski et al. 2003). To establish the relationship between  
179 topology and density and pumping energy, the base demand was increased by a global multiplier  
180 of three (1,200 lpcd) to represent peak hour water usage for the simulation. While peak hour  
181 demands are not representative of annual energy consumption patterns, they did allow for a  
182 clearer comparison of energy use across neighbourhoods.

183

184 A node in each neighbourhood was connected to a pump and water supply reservoir, located at  
185 the junction where the neighbourhood would be connected to a main road with a feeder main.  
186 Each pump had a pump curve with points  $Q_1=0, H_1 = 4/3 H$  and  $Q_2 = 2Q, H_2=0$ . The flow  $Q$  was  
187 set at double the total base average demand of each neighbourhood (approximately 21 lps), a  
188 value sufficiently large to accommodate the increase in demand due to the global multiplier. It is  
189 noted that no Boolean logic rules were used to control the pump and reservoir in the networks  
190 considered. As such, the pumping energy use values reported in this paper do not include the  
191 added energy associated with pump switches. Further, changes in electricity prices were not  
192 considered because the energy analysis is a snapshot in time and does consider energy use over a  
193 long-term period. The head  $H$  was set at the minimum value required to ensure that the lowest  
194 pressure head at any node is 40 m (Great Lakes-Upper Mississippi River Board of State and  
195 Provincial Health and Environmental Managers, 2012). All pipe diameters were assigned a  
196 starting value of 150 mm (6 inches), with a Hazen-Williams C factor of 130 to represent new  
197 ductile-iron pipe (Prosser et al. 2013). If the velocity in the pipe exceeded 1.5 m/s (5 ft/s) during  
198 hydraulic analysis, the pipe diameter was increased to the next commercially-available size until  
199 its velocity was below this threshold value.

200

201 Relationship Between Network Connectivity and Pumping Energy Use: To examine the role of  
202 pipe connectivity on pumping energy, the internal connectivity measure developed by Knaap et  
203 al. (2007) was used to quantitatively characterize the networks. The internal connectivity of a  
204 neighbourhood, was defined by Knaap (2007) as

$$205 \quad \text{Internal Connectivity} = \frac{\# \text{Intersections}}{\# \text{Intersections} + \text{Dead Ends}}$$

206 where a high degree of connectivity is represented with a large numerical value of the internal  
207 connectivity index. The maximum value for the internal connectivity index is 1, where no cul-de-  
208 sacs are present in the neighbourhood.

209

210 With a quantitative description of topology established, the degree of correlation between  
211 connectivity and pumping energy was quantified with Spearman's rank correlation coefficient  
212 (Spearman's  $\rho$ ). Spearman's rank is a nonparametric measure of the correspondence between two

213 ranked monotonic variables (Myers et al. 2010). A Spearman coefficient of -1 or +1 indicates a  
214 perfect negative or positive monotonic relationship between the two variables. The Spearman  
215 correlation coefficient,  $\rho$  is computed from the equation:

$$216 \quad \rho = 1 - \frac{6 \sum d_i^2}{n(n^2 - 1)}$$

217 where  $d_i = x_i - y_i$ , with  $x_i$  and  $y_i$  as the ranks of the variables  $X_i$  and  $Y_i$ , and  $n$  is the sample size.

218 Hypothesis testing is conducted with the null hypothesis  $H_0: \rho = 0$  and the alternative hypothesis

219  $H_A: \rho \neq 0$ . Significance is tested with the Student 't' statistic,

$$220 \quad t = \frac{r\sqrt{n-2}}{\sqrt{1-r^2}}$$

221 where  $r$  is the sample correlation coefficient.

222

## 223 **Results and Discussion**

### 224 *Impact of Street Topology and Population Density on Energy Use*

225 For each energy component (embodied energy and pumping energy), the neighbourhood  
226 scenarios were compared across topology (density held constant), and then across population  
227 density (topology was fixed).

228

229 Comparison of Embodied Energy Across Topologies: Figure 3 reports the per capita embodied  
230 energy use for each neighbourhood at high, medium, and low densities, as well as for each base  
231 scenario, where the original street lengths and lot sizes of the neighbourhood were held constant.

232 Embodied energy is proportional to the total length of pipe, except for in the instances where  
233 pipe diameter has been upgraded to meet the maximum velocity criterion. WP-3 was the only  
234 neighbourhood that required an increase in diameter. This increase occurred for only one pipe  
235 and was applied to all density scenarios. As a result, the main driving force for embodied energy  
236 use in this investigation is pipe length. Figure 3 indicates that with the exception of  
237 neighbourhood WP-3, gridiron neighbourhoods generally have a lower embodied energy  
238 requirement than warped parallel or cul-de-sac/loop neighbourhoods. This result is confirmed by  
239 the fact that almost all warped parallel and cul-de-sac/loop networks in this investigation were  
240 longer than the gridiron networks.

241

242 The marked differences in embodied energy across the topologies considered is explained by the  
243 extent to which green space is included in the three urban forms. Neighborhoods with warped  
244 parallel and cul-de-sac/loop topologies often have buffer zones that separate individual lots and  
245 tracts of land from the main road (Southworth and Owens 1993). This means that an additional  
246 length of pipe is needed to connect unhoused areas, requiring a longer total length of pipe for the  
247 same number of lots, and increasing embodied energy requirements. In gridiron neighbourhoods,  
248 lots are usually closely space to each other and to the road and all available space within the  
249 neighbourhood is developed. This tends to minimize the length of pipe needed to service the  
250 neighborhood population and reduce the embodied energy requirements.

251

252 Comparison of Embodied Energy Across Densities: Figure 4 plots embodied energy against  
253 density for each topology. The warped parallel and cul-de-sac/loop neighbourhoods see an  
254 increase in embodied energy that ranges between 1.5 and 1.9 kWh/c per m<sup>2</sup> increase in lot area,  
255 with the exception of WP-3, as population density is decreased. Gridiron neighbourhoods see a  
256 slightly smaller increase of 1.2 kWh/c per m<sup>2</sup>, with the exception of GR-3, as population density  
257 is decreased. Further, as the population density is decreased, the increase in pipe length, and the  
258 corresponding embodied energy, is greater for warped parallel and cul-de-sac/loop networks than  
259 for gridiron networks, to accommodate the increase in lot area to accommodate lower densities.

260

261 Increasing the area of narrow lots while maintaining their aspect ratios increases frontage  
262 slightly, with the major increase in dimension seen in the depth of an entire row of lots. On the  
263 other hand, increasing the area of wide lots means that each lot contributes a major increase in  
264 frontage. As a result, moving from high to low density, neighbourhoods with wider lots  
265 experienced greater increases in pipe length than those with narrower lots; this resulted in greater  
266 increases in embodied energy. The topologies GR-3 and WP-3 saw lower increases in embodied  
267 energy across density than the other neighbourhoods in their respective topology categories. This  
268 is because both GR-3 and WP-3 neighbourhoods have narrow rectangular lots (with 10 m  
269 frontages) and they are not sensitive to density changes.

270

271 Comparison of Pumping Energy Across Topologies: Figure 5 reports the peak hour per capita  
272 pumping energy use of each neighbourhood at high, medium and low densities, as well as the

273 pumping energy use for each base neighbourhood. The results suggest that gridiron  
274 neighbourhoods have the lowest pumping energy use compared to the other topologies. This is  
275 because gridiron networks are highly interconnected, which allows flow to be distributed more  
276 evenly across the network with lower friction losses. It is also noted that the energy use values  
277 for pipe layouts within the gridiron topology and pipe layouts within the cul-de-sac/loop  
278 topology are clustered together. However, the energy use values for pipe layouts within the  
279 warped parallel topology span a wide range. In addition, the energy use values for WP-2 and  
280 WP-3 are greater than those of the cul-de-sac/loop neighbourhoods, even though warped parallel  
281 pipe layouts are slightly more connected than cul-de-sac/loop pipe layouts.

282

283 To further examine the role of pipe connectivity on pumping energy, the connectivity measure  
284 developed by Knaap et al. (2007) was used to quantitatively characterize the networks. Table 3  
285 reports the connectivity index of each network. Gridiron networks have no dead-ends and thus  
286 have the highest index value. Connectivity decreases as one moves from warped parallel to cul-  
287 de-sac/loop networks. This result confirms the trend of decreasing connectivity observed by  
288 Southworth and Owens (1993).

289

290 For each neighbourhood scenario, the Spearman's rank correlation coefficient was calculated for  
291 the correlation between network connectivity and pumping energy and are shown in Table 4. The  
292 base models exhibit a negative correlation ( $\rho = -0.750$ ) between the connectivity index and  
293 pumping energy. However, when comparing neighbourhoods at the same density, the correlation  
294 between the connectivity index and pumping energy is lower ( $\rho = -0.583$ ), suggesting that the  
295 degree of network connectivity is likely not the primary driving force behind differences in  
296 pumping energy consumption.

297

298 Flow Splitting: To better understand the differences in pumping energy consumption, the flow  
299 paths of each neighbourhood scenario were evaluated. Recall that pumping energy is required to  
300 overcome three sources of energy loss—increases in elevation, local losses, and losses due to pipe  
301 friction—while fulfilling the minimum pressure head criterion of 40 m.

302

303 In this study, the same minimum pressure head criterion was applied to all networks and no  
304 change in elevation or local losses were considered. As a result, pumping energy differences are  
305 linked to friction loss along pipes which is dependent on pipe length, flow, roughness, and  
306 diameter. Since pipe roughness and diameter values were the same for all networks (with the  
307 exception of one pipe in WP-3), friction loss is mainly driven by pipe length and flow. Because  
308 each network is connected to a single water source, the entire neighbourhood demand flow must  
309 pass through this area of connection to the source reservoir. Thus pipes closest to the source  
310 convey the largest flows in the network and consequently, friction losses in this area are greatest.

311  
312 For each network, pipes carrying more than one third of the total neighbourhood demand were  
313 identified. As expected, all pipes that met this criterion were located near the water reservoir.  
314 The length of pipes that carried more than one third of total demand in each neighbourhood were  
315 summed to obtain a metric named “total high flow pipe length” in each network. Spearman's  $\rho$   
316 values for the correlation between total high flow pipe length and pumping energy are indicated  
317 in Table 4. For comparison, the Spearman's  $\rho$  values for the correlation between total pipe length  
318 and pumping energy is indicated in Table 4. These results show that pumping energy is more  
319 strongly correlated to total high flow pipe length than to the connectivity index or to the total  
320 pipe length of the network.

321  
322 These results suggest that pumping energy use is affected by how quickly large flows that leave  
323 the water reservoir are split into smaller flows. The more numerous the intersections are in the  
324 area surrounding the water source or connection to transmission pipes, the shorter the distance  
325 large flows must travel before being split into smaller flows with lower friction losses. In other  
326 words, while “global” network connectivity may not affect pumping energy use significantly, the  
327 “local” connectivity of the pipes near the water source has an important impact on pumping  
328 energy use.

329  
330 Figure 2 indicates that WP-2 and WP-3 have very few intersections near their water source  
331 connection. Although these networks are better connected downstream, the low connectivity near  
332 their water reservoirs drives their pumping energy use past those of the cul-de-sac/loop networks.

333 WP-1 had significantly lower pumping energy use because the area around the network water  
334 reservoir is well connected.

335  
336 As mentioned above, warped parallel and cul-de-sac/loop topologies were popular at a time  
337 when it was common practice to incorporate green buffer zones to separate the main line  
338 connection and the neighbourhood proper. So because of this buffer distance, warped parallel  
339 and cul-de-sac/loop networks carry high flows for longer distances. On the other hand, gridiron  
340 neighbourhoods tend to be directly integrated into heavily urbanized areas, and flows that enter a  
341 gridiron neighbourhood has only to be conveyed a short distance before being bifurcated into  
342 smaller flows along distribution mains.

343  
344 Comparison of Pumping Energy Across Densities: Figure 6 plots pumping energy against  
345 population density for each topology. As as population density is decreased, the warped parallel  
346 and cul-de-sac/loop neighbourhoods see small increases in pumping energy use and the gridiron  
347 neighbourhoods see almost no increase in pumping energy use. This indicates that pumping  
348 energy use in gridiron neighbourhoods is less sensitive to changes in density than in the other  
349 topologies. Since pumping energy use is linked strictly to frictional losses in pipes in this paper,  
350 then it follows that the sensitivity of pumping energy to density is thus linked to the magnitude  
351 of change in pipe lengths across densities. The distribution of flows along water mains was fixed  
352 across all densities in each neighbourhood.

353  
354 A moderate correlation was found between the change in pumping energy across densities and  
355 the change in total pipe length across densities (Spearman's  $\rho = 0.450$ ,  $H_0: \rho = 0$  rejected with a  
356 confidence level  $< 80\%$ ). However, a stronger positive correlation was found between the change  
357 in pumping energy across densities and the change in high flow pipe length across densities  
358 (Spearman's  $\rho = 0.933$ ,  $H_0: \rho = 0$  rejected with a confidence level of  $99.9\%$ ). From earlier  
359 analysis, it was found that warped parallel and cul-de-sac/loop neighbourhoods tend to have  
360 longer high flow pipe lengths due to the lower connectivity in the area near their water  
361 reservoirs. Moving from high to low density, these high flow pipes experience a larger increase  
362 in length (and thus a larger increase in friction losses) than the shorter pipe segments found near  
363 the water source connection of gridiron networks. As a result, neighbourhoods with low

364 connectivity at their water source connection points are more sensitive to changes in density than  
365 neighbourhoods with higher connectivity at their connection points.

366  
367 In this study, different neighborhood topologies were systematically paired with different levels  
368 of population density to examine energy use. In reality, each topology tends to be associated with  
369 a certain “native” density in reality. Further, the neighbourhoods in this investigation were  
370 assumed to be homogeneously residential when in reality, older gridiron neighbourhoods (and  
371 some neotraditional neighbourhoods) tend to have more diversity in land use than newer cul-de-  
372 sac/loop subdivisions. This non-homogenous nature of actual neighborhoods can result in a  
373 divergence of water demand patterns from a neighborhood where land-use is considered  
374 homogenous. As mentioned above, all neighborhood topologies were fixed at a constant  
375 elevation to compare their energy use fairly. In reality, each neighborhood has a unique  
376 topography and corresponding static lift that will create a difference in energy requirements  
377 across neighborhoods. For the sake of a fair comparison, this was not captured in this paper.

378  
379 This paper has highlighted how the geographic form of neighborhoods mediates the link between  
380 water provision and energy use in the urban water-nexus. The neotraditional neighbourhood  
381 forms has been identified by researchers as having the potential to reduce energy use in urban  
382 areas (Grammenos and Grant 2008; Conway 2009). The neotraditional neighbourhood form  
383 integrates the “traditional” gridiron form as the basis for its street layout while incorporating  
384 additional design tenets related to “traditional” land use mix, income diversity, and architecture  
385 (Grammenos and Grant 2008; Conway 2009). Examples of the neotraditional form include the  
386 New Urbanist and Fused Grid topologies that tend to mimic the gridiron pattern by connecting  
387 pedestrian walkways, green space, and cul-de-sacs. However, whether neotraditional  
388 neighborhood forms are successful at lowering energy requirements relative to their conventional  
389 warped parallel and cul-de-sac/loop counterparts will turn on whether they can maintain large  
390 population densities and short block lengths to achieve strong “economies of water provision  
391 scales” like the traditional gridiron form.

392  
393 **Summary and Conclusions**

394

395 This paper examined the relationship between urban form and energy use in water supply and  
396 distribution systems through the use of neighbourhood scenarios. Urban form was defined in  
397 terms of street topology and population density. Energy use was evaluated in two components—  
398 embodied energy and pumping energy. Neighbourhood scenarios were created through a  
399 combination of three historical topologies (gridiron, warped parallel, and cul-de-sac/loop) and  
400 three population densities (high, medium, and low).

401  
402 Per capita embodied energy requirements were lower in gridiron neighbourhoods than in the  
403 warped parallel and cul-de-sac/loop neighbourhoods with longer pipe lengths. Pumping energy  
404 was only weakly correlated to the neighbourhood's overall connectivity. Instead, pumping energy  
405 was more strongly correlated to the connectivity of the area surrounding the neighbourhood's  
406 water source. Flows entering a gridiron neighbourhood tended to split into smaller flows more  
407 quickly due to high connectivity near its water source. The warped parallel and cul-de-sac/loop  
408 neighbourhoods had higher pumping energy requirements because of their longer length of pipe  
409 that conveyed high flows.

410

#### 411 **References**

412 Aubuchon CP, Roberson JA (2014) Evaluating the embedded energy in real water loss. J  
413 American Water Works Association 106(3): E129–E138

414

415 Autodesk Inc (2011) AutoCAD Software.

416

417 Cabrera E, Pardo MA, Cobacho R, Cabrera Jr, E (2010) Energy audit of water networks. J of  
418 Water Resources Planning and Management 136(6): 669–677

419

420 City of Miamisburg (2013) Planning and zoning code of the City of Miamisburg, American  
421 Legal Publishing Corporation, Cincinnati, Ohio, pp. 336.

422

423 Conway, T. (2009). Local environmental impacts of alternative forms of residential  
424 development. *Environment and Planning B: Planning and Design*, 36(5), 927–943.

425

426 Domene E, Sauri D (2006) Urbanization and water consumption: Influencing factors in the  
427 metropolitan region of Barcelona. In: *Urban Studies*, 43(9): 1605–1623.  
428

429 Ellis C (2002) The New Urbanism: Critiques and rebuttals. *J of Urban Design* 7(3): 261–291.  
430

431 Environment Canada (2011) 2011 municipal water use report. Government of Canada, Gatineau,  
432 QC. [https://www.ec.gc.ca/doc/publications/eau-water/COM1454/long\\_descrip-eng.htm](https://www.ec.gc.ca/doc/publications/eau-water/COM1454/long_descrip-eng.htm).  
433 Accessed July 16, 2019  
434

435 Farmani R, Butler D (2014) Implications of Urban Form on Water Distribution Systems  
436 Performance. *Water Resources Management*, 28: 83-97.  
437

438 Filion YR (2008) Impact of urban form on energy use in water distribution systems. *J of*  
439 *Infrastructure Systems* 14(4): 337–346  
440

441 Friedman K, Heaney JP, Morales M, Palenchar JE et al (2013) Predicting and managing  
442 residential potable irrigation using parcel-level databases. *J American Water Works Association*  
443 105(7): E372–E386  
444

445 Goldstein R, Smith W (2002) Water & sustainability: US electricity consumption for water  
446 supply & treatment-the next half century. Electric Power Research Institute, Palo Alto, CA, pp.  
447 57.  
448

449 Grammenos, F., & Grant, D. (2008). *Breaking ground: A fused-grid neighbourhood*  
450 *in Calgary*. Canadian Mortgage and Housing Corporation Report, 1–8.  
451

452 Google Inc (2013) Google Earth. <https://www.google.com/earth/>. Accessed July 16, 2019  
453

454 Grammenos F, Grant D (2004) Applying fused-grid planning in Stratford, Ontario. Canadian  
455 Mortgage and Housing Corporation Report. Ottawa, ON, pp. 6.  
456

457 Grammenos F, Grant, D (2008) Breaking ground: A fused-grid neighbourhood in Calgary.  
458 Canadian Mortgage and Housing Corporation Report. Ottawa, ON, pp. 8.  
459  
460 Great Lakes Upper Mississippi River Board of State and Provincial Health and Environmental  
461 Managers (2012) Recommended standards for water works. Albany, NY, pp. 123.  
462  
463 Huang C, Li Y, Li X, Wang H, Yan J, Wang X, Wu J, Li F (2018) Understanding the water-  
464 energy nexus in urban water supply systems with city features. *Energy Procedia*, 152(2018),  
465 265-270.  
466  
467 Jia N, Sitzenfrei R, Rauch W, Liang S, Liu Y (2019) Effects of Urban Forms on Separate  
468 Drainage Systems: A Virtual City Perspective. *Water*, 11, 758-776.  
469  
470 Knaap GJ, SongY, Nedovic-Budic Z (2007) Measuring patterns of urban development: New  
471 intelligence for the war on sprawl. *J Local Environment* 12 (3): 239–257  
472  
473 Ministry of the Environment (2008) *Design Guidelines for Drinking-Water Systems*, Queen’s  
474 Publisher, Toronto, Ontario, Canada.  
475  
476 Myers JL, Well A, Lorch RF (2010) Research design and statistical analysis. Routledge, New  
477 York, NY, pp. 832.  
478  
479 Prosser ME, Speight VL, Fillion YR (2013). Life-cycle energy analysis of performance versus  
480 age-based pipe replacement schedules. *J American Water Works Association* 105 (12): E721–  
481 E732  
482  
483 Rossman LA (2000) EPANET 2: User’s manual. US Environmental Protection Agency.  
484 Cincinnati, OH  
485

486 Sakrison RG (1997) Summer water use in compact communities: the effect of small lots and  
487 growth management plans on single-family water use in King County, Washington (PhD thesis).  
488 University of Washington.  
489

490 Sanders KT, Webber ME (2012) Evaluating the energy consumed for water use in the United  
491 States. *Environmental Research Letters* 7 (3): 1–11  
492

493 Southworth M (1997) Walkable suburbs: An evaluation of neotraditional communities at the  
494 urban edge. *J of the American Planning Association* 63 (1): 28–44  
495

496 Southworth M, Owens P M (1993) The evolving metropolis: Studies of community,  
497 neighborhood, and street form at the urban edge. *J of the American Planning Association* 59:(3)  
498 271–287  
499

500 Trudeau D (2013) A typology of New Urbanism neighborhoods. *J of Urbanism: International*  
501 *Research on Placemaking and Urban Sustainability* 6:(2) 113–138  
502

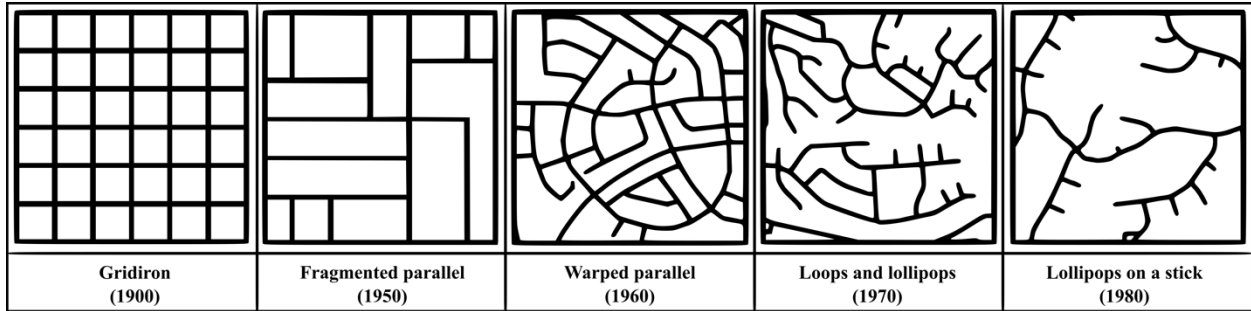
503 Van Lare, P (2005) How thirsty is your community? *Zoning Practice* 5. American Planning  
504 Association, pp. 8.  
505

506 Walski TM, Chase DV, Savic DA, Grayman WM, Beckwith S, Koelle E et al (2003) *Advanced*  
507 *water distribution modelling and management*. Haestad Press.  
508

509 Wong H, Speight V, Filion Y (2017) Impact of Urban Development on the Energy Use of a  
510 Distribution System. *Journal of American Water Works Association*, 109(1): E10-E18  
511  
512

513  
514  
515  
516

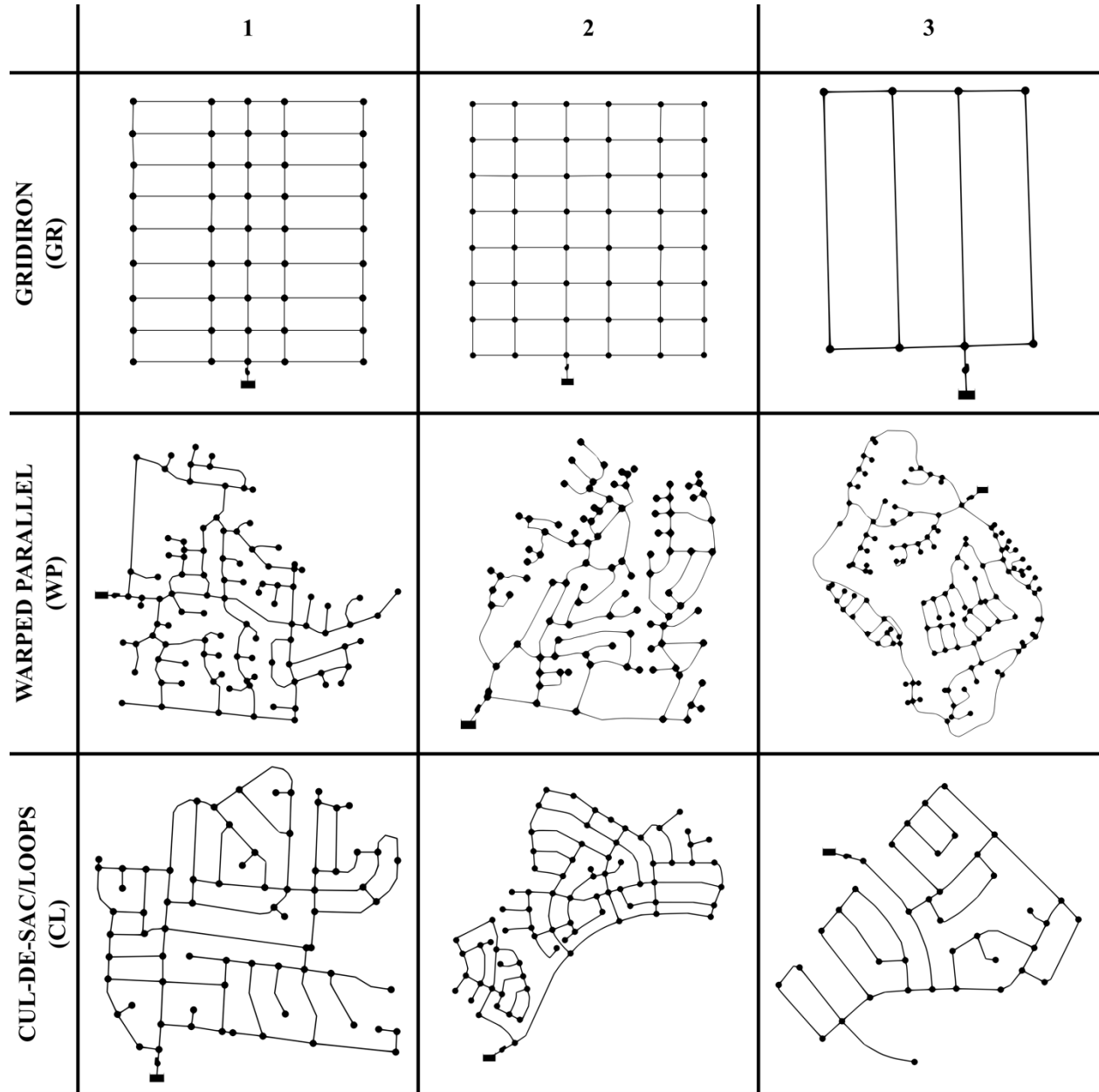
**Fig 1** Neighbourhood street patterns adapted from Southworth and Owens (1993).  
(Images are not to scale)



517  
518  
519  
520  
521  
522  
523

524  
525  
526

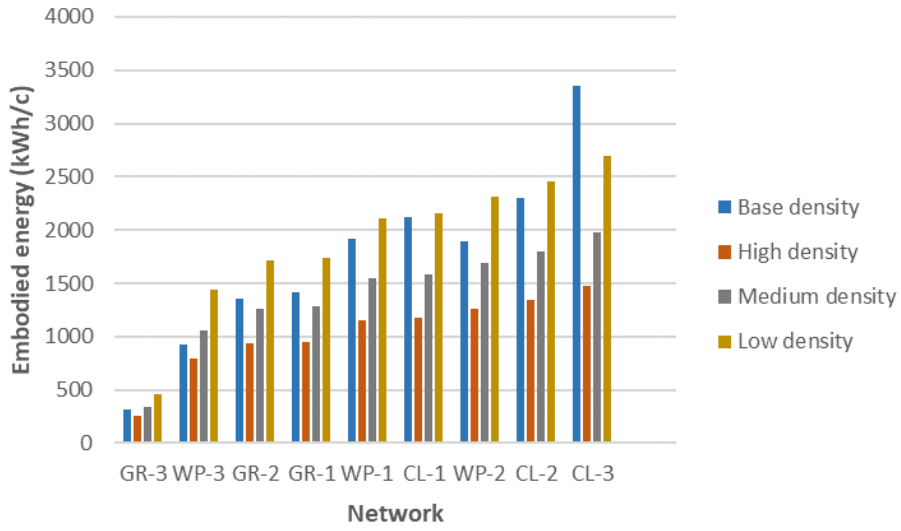
**Fig 2** Neighbourhood layouts for each topology category. (Images are not to scale)



527  
528  
529

530  
531  
532

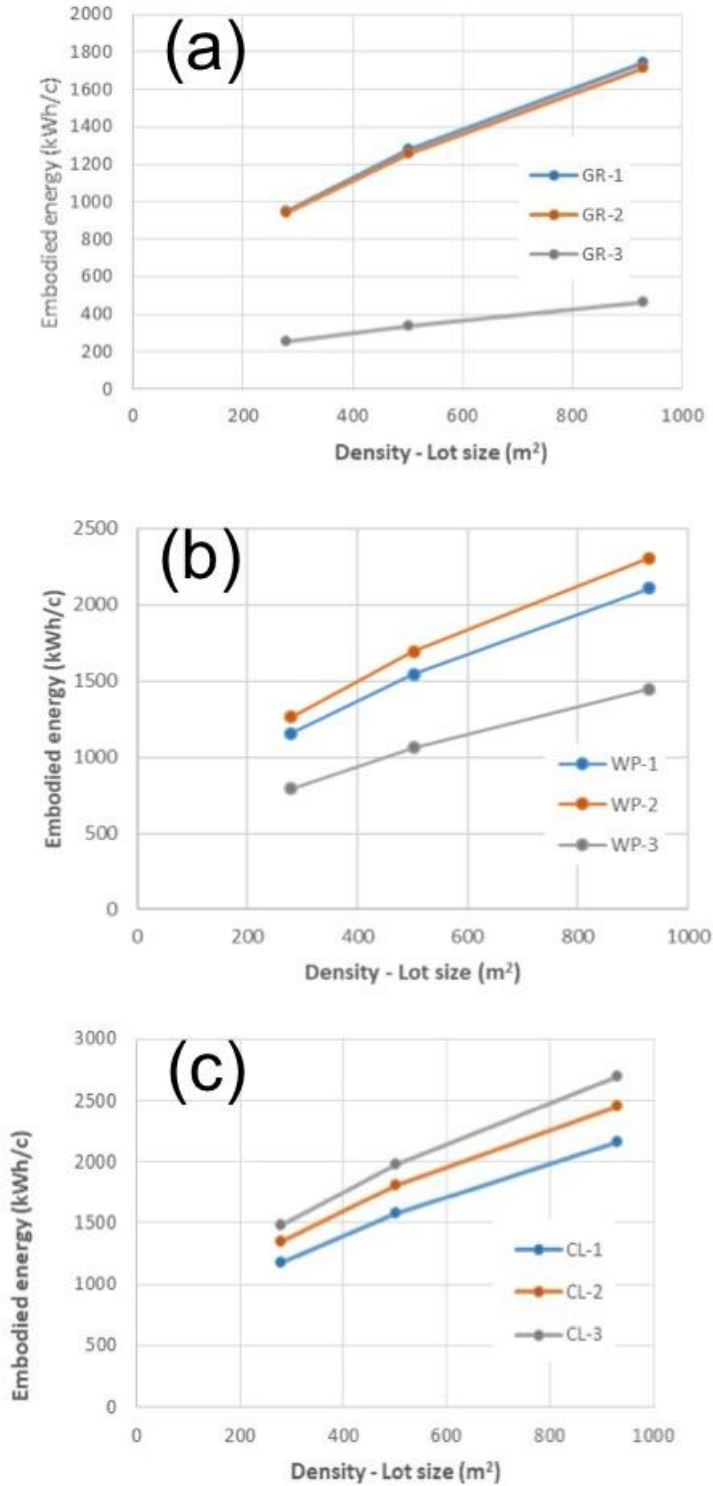
**Fig 3** Embodied energy vs topology for high, medium, low, and base density neighbourhoods



533  
534

535  
536  
537  
538

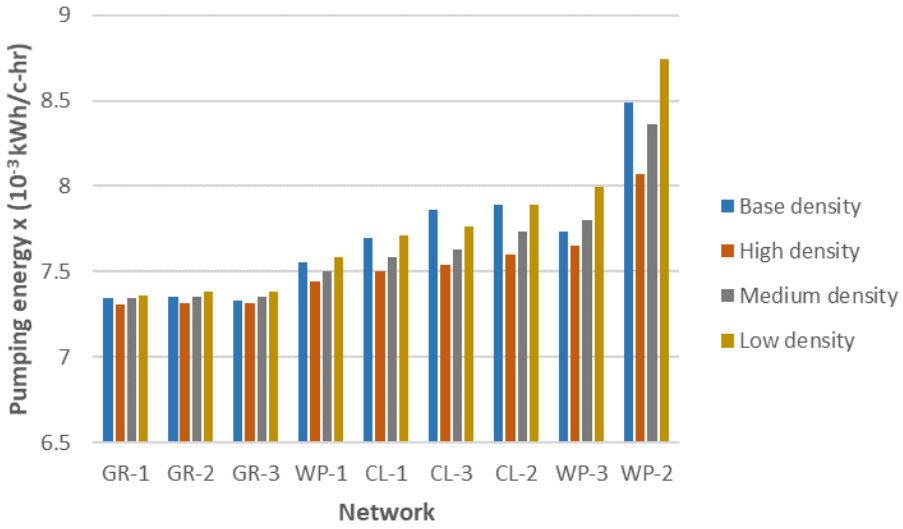
**Fig 4** Embodied energy vs density for a) gridiron, b) warped parallel, and c) cul-de-sac/loop, neighbourhoods. The density values correspond to the lot areas for high, medium, and low density neighbourhoods.



539

540  
541  
542

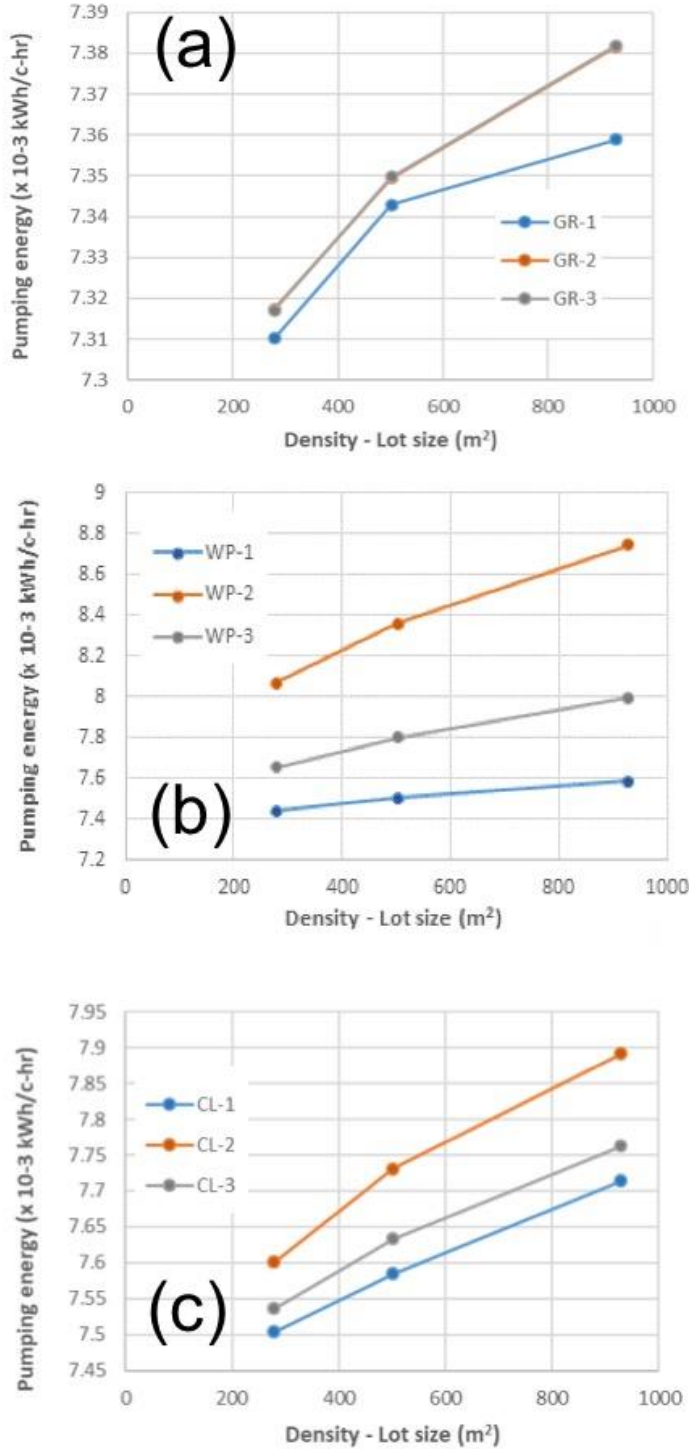
**Fig 5** Pumping energy vs topology for high, medium, low, and base density neighbourhoods



543  
544

545  
546  
547  
548

**Fig 6** Pumping energy vs density for a) gridiron, b) warped parallel, and c) cul-de sac/loop neighbourhoods. The density values correspond to the lot areas for high, medium, and low density neighbourhoods.



549  
550

551

552 **Table 1.** Lot areas for high, medium, and low densities

<b>Density</b>	<b>Lot Size (m<sup>2</sup>)</b>	<b>Lot Size (ft<sup>2</sup>)</b>	<b>Associated Base Neighbourhoods</b>
High	279	3,000	GR-3, WP-3
Medium	502	5,400	GR-1, GR-2, WP-2
Low	929	10,000	WP-1, CL-1, CL-2, CL-3

553

554

555 **Table 2.** Network parameter inputs for hydraulic modelling

<b>Network Parameter</b>	<b>Input</b>
Reservoir water level	0 m
Junction elevations	0 m
Pump curve flow, $Q$	21 lps
Pump curve head, $H$	Dependent on hydraulic criteria
Pump efficiency, $\eta$	75%
Pipe diameter	150 mm; dependent on hydraulic criteria
Pipe roughness (Hazen-Williams C)	130
Base per capita demand	400 lpcd

556  
557

558 **Table 3.** Connectivity index value for each neighbourhood

<b>Neighbourhood</b>	<b>Connectivity Index</b>
GR-1	1.00
GR-2	1.00
GR-3	1.00
LL-1	0.40
LL-2	0.45
LL-3	0.35
WP-1	0.75
WP-2	0.74
WP-3	0.85

559

560

561  
562  
563  
564

**Table 4.** Correlation between pumping energy and network connectivity, high flow pipe length, and total pipe length

Density	Network Connectivity		High Flow Pipe Length		Total Pipe Length	
	Spearman's $\rho$	CL*	Spearman's $\rho$	CL*	Spearman's $\rho$	CL*
Base	-0.750	98%	0.883	99.8%	0.700	95%
High	-0.583	90%	0.917	99.9%	0.517	80%
Medium	-0.583	90%	0.967	99.9%	0.467	< 80%
Low	-0.583	90%	0.933	99.9%	0.450	< 80%

565  
566  
567

\* CL = Confidence level.